Supramolecular Hydrogels Based on L-Phenylalanine Derivatives with a Positively Charged Terminal Group

by **Xin-Jian Fu***[a])[b]), **Hua Zhang**[b]), **Si-Kai Zhou**[b]), **Shao-Bing Liu**[b]), **Fu-Quan Guo**[b]), **Hong Wang**[a]), and **Ya-Jiang Yang***[a])

[a]) Department of Chemistry and Chemical Engineering, Huazhong University of Science and Technology, Wuhan 430074, P. R. China

[b]) Department of Materials Engineering, Luoyang Institute of Science and Technology, Luoyang 471023, P. R. China (phone: +86-379-65928203; fax: +86-379-65928196; e-mail: fuxinjian@126.com)

A new hydrogelator based on L-phenylalanine with a long hydrophobic chain and positively charged terminus was synthesized, and its gelation behavior in H_2O was investigated. Polarized optical microscopy (POM), field emission scanning electron microscopy (FE-SEM), and X-ray diffraction (XRD) results indicate that the hydrogelator self-assembles into fibres-like aggregates which then lead to the formation of a hydrogel. ^{1}H-NMR and CD spectra of hydrogels and aqueous solution revealed that intermolecular H-bonding between the amide groups was the driving force for gelation. A luminescence study, in which ANS (8-anilinonaphthalene-1-sulfonic acid) was used as a probe, indicated that the hydrophobic interactions between long chains were the driving force for gelation. Consequently, it was proved that the hydrogelator self-assembles into fibre-like aggregates and then forms supramolecular hydrogels through the H-bonding and hydrophobic interactions.

Introduction. – In the past decades, organogels, in which organic solvents are gelled by low-molecular-weight compounds (organogelators), have attracted much attention owing to their unique features and potential applications for new organic soft materials [1]. Organogelators can self-assemble into supramolecular aggregates through intermolecular interactions, such as H-bonding, $\pi-\pi$ stacking, *Van der Waals* attractions, coordination, and charge transfer. The solvent molecules are immobilized by capillary forces in a three-dimensional network and lead to the gelation of organic solvents. Although quite a few low-molecular-weight organogelators and their applications have been reported, the study of low-molecular-weight hydrogelator (LMWH) has been very limited [2]. Unlike traditional polymer hydrogels, which are H_2O-swollen crosslinked polymers, the LMWHs are preferred because of their rapid response to external stimuli and thermoreversible nature, due to noncovalent interactions. For the application of supramolecular hydrogels for biological use, their biocompatibility and responsiveness are indispensable [3]. Furthermore, hydrogelators formed in the presence of even a limited amount of additional organic solvent would restrict their application in biological systems [4]. Hydrogelators can also gelate in H_2O which is interesting according to the essential criteria for biological use [5].

For an appropriate hydrogelator, the presence of both hydrophilic and hydrophobic groups within the same molecule is an important requirement to aggregate in an ordered fashion to induce immobilization of H_2O [6]. Amphiphilic molecules,

especially amino acid derived hydrogelators, not only have such characteristics but also are biodegradable and have low toxicity. *Suzuki* and co-workers synthesized some amino acid derived hydrogelators, such as valine, isoleucine, and lysine derived with positively charged pyridinium or imidazolium moieties as terminal groups, which can gelatinize H_2O [7]. *Motulsky et al.* reported the gelation of vegetable oil and H_2O in the presence of six different amphiphilic gelators based on L-alanine derivatives. They also reported the formation of hydrogels through subcutaneous injections in rats and the biodegradation and biocompatibility of hydrogels [6a]. In our previous research works, we have synthesized an amphiphilic hydrogelator based on L-phenylalanine derivatives and investigated the formation mechanism of supramolecular hydrogels [8].

In this work, an amphiphilic hydrogelator based on L-phenylalanine, *N*-octadecyl-N^{α}-[6-(pyridinium-1-yl)hexanoyl]-L-phenylalaninamide bromide (**NP18PB**), was synthesized and characterized. The formation mechanism of supramolecular hydrogels in the presence of **NP18PB** was investigated by using ^{1}H-NMR, polarized optical microscopy (POM), field emission scanning electron microscopy (FE-SEM), fluorescence, X-ray diffraction (XRD), and circular dichroism (CD).

Results and Discussion. – 1. *Synthesis of* **NP18PB** (*Scheme*). The starting material (4*S*)-4-benzyl-1,3-oxazolidine-2,5-dione (**L-Phe-NCA**) was synthesized according to a reported procedure [9]. Octadecylamine and **L-Phe-NCA** were reacted in CH_2Cl_2 at 40°. The product *N*-octadecyl-L-phenylalaninamide (designated as **C_{18}Phe**) was then reacted with 6-bromohexanoyl chloride in the presence of Et_3N to yield N^{α}-(6-bromohexanoyl)-*N*-octadecyl-L-phenylalaninamide (designated as **NP18**). **NP18** was refluxed in pyridine leading to *N*-octadecyl-N^{α}-[6-(pyridinium-1-yl)hexanoyl]-L-phenylalaninamide bromide (**NP18PB**).

2. *Hydrogelation Properties.* The hydrogelation properties of **NP18PB** and its minimum gel concentration (MGC) necessary for the gelation of H_2O was investigated and evaluated by the 'stable to inversion of a test tube' method [10]. Dissolution of **NP18PB** in H_2O by heating to 80° and subsequent cooling to room temperature led to gelation at concentrations of 1.2 wt-% and above, and a visible and transparent hydrogel was observed. Each hydrogelator molecule has thus the ability to immobilize *ca.* 3100 H_2O molecules at room temperature. Furthermore, the hydrogel formed by **NP18PB** (1.2 wt-%) was observed to be stable at room temperature over a period of one year.

Fig. 1 shows gel-to-solution transition temperatures (T_{GS}) of supramolecular hydrogels which formed with different concentrations of **NP18PB**, as determined by dropping ball measurements. As shown in *Fig. 1*, while increasing the MGCs from 1.5 to 3.5 wt-%, T_{GS} of hydrogels increased from 40° to 68° rapidly, whereas the T_{GS} of hydrogels increased from 68° to 73° slowly as the MGCs increased from 3.5 to 4.5 wt-%. The higher stability of hydrogels at higher gelation concentration indicates that self-assembly in the gel state is driven by strong intermolecular, noncovalent interactions [5b].

3. *Field Emission Scanning Electron Microscopy* (FE-SEM) *and Polarized Optical Microscope* (POM). To obtain visual insights into the aggregation mode of these gelators in hydrogels, we took POM and FE-SEM images of the hydrogel. *Fig. 2* shows the FE-SEM and POM images of supramolecular hydrogels formed by **NP18PB**. As

Scheme. *Synthesis of* **NP18PB**

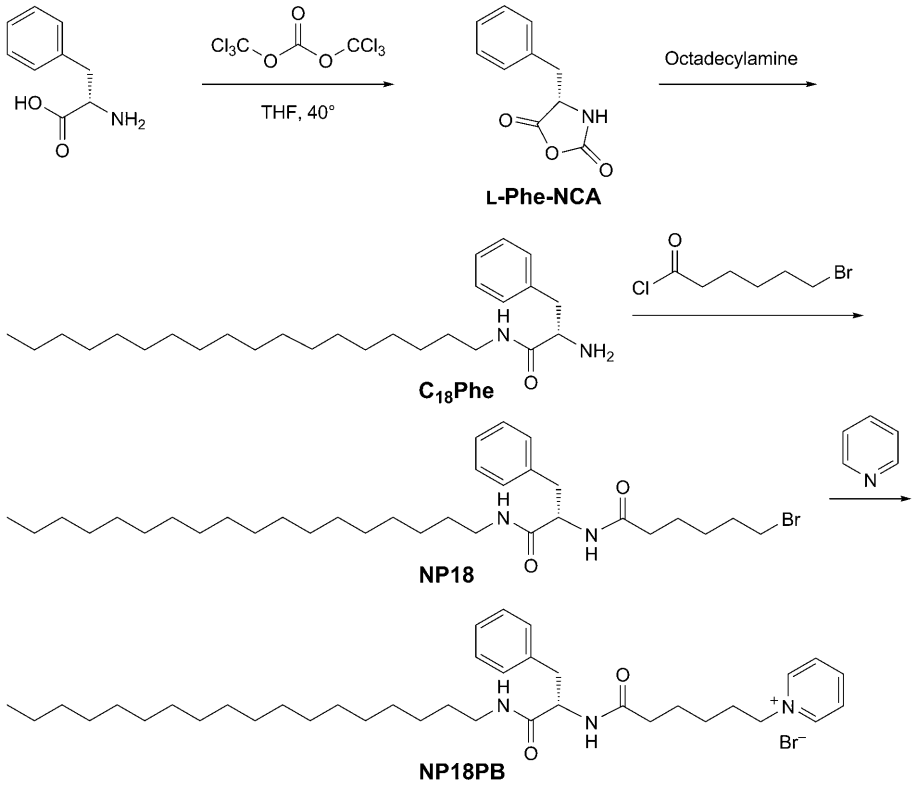

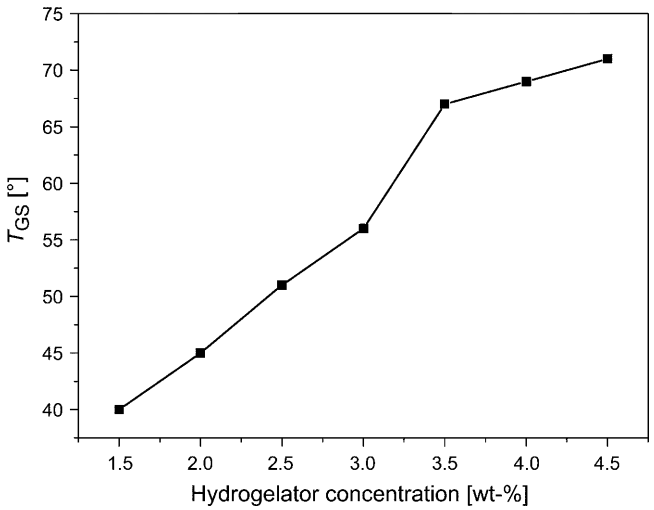

Fig. 1. *Variation of the* T_{GS} *with the concentration of* **NP18PB**

shown in *Fig. 2,a*, **NP18PB** can self-assemble in deionized H_2O and form nanofibers with a diameter of *ca.* 30–50 nm (*Fig. 2,a*). Furthermore, typical fiber-like crystallites

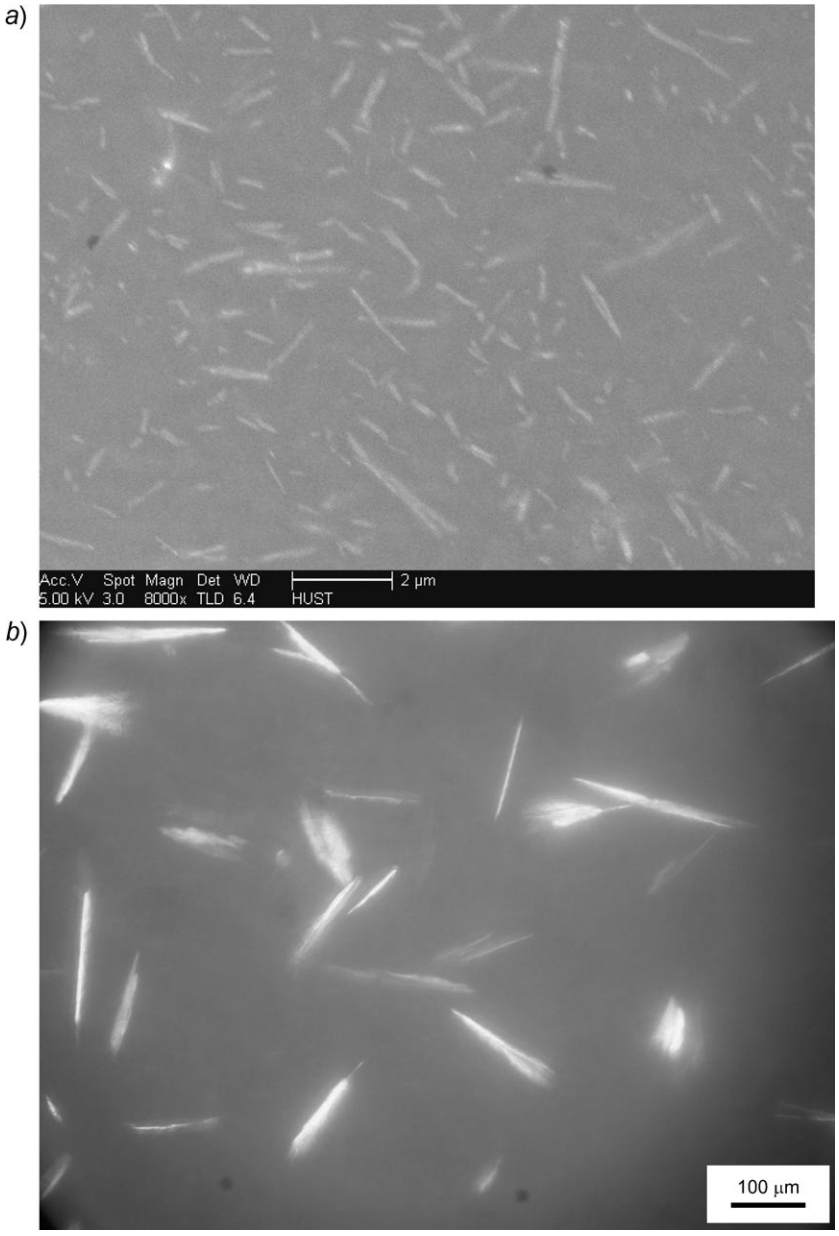

Fig. 2. *a*) *Field Emission Scanning Electron Micrographs* (FE-SEM) *of dried gels formed by 3.0 wt-% of gelator in deionized H_2O, magnified by 8000. b*) *Polarizing optical micrographs* (POM) *of hydrogels formed by 4.0 wt-% of gelator in deionized H_2O, magnified by 400.*

with a diameter of *ca.* 30 μm were observed as shown in *Fig. 2,b*. These results indicate that the hydrogelator can self-assemble into fiber-like aggregates and H_2O molecules are entrapped in the three-dimensional network by capillary forces, which lead to the formation of stable hydrogels.

4. *^{1}H-NMR Spectra.* To obtain information on the intermolecular H-bonding interaction between the amide groups, the ^{1}H-NMR study was performed by using 1.5 wt-% **NP18PB** in (D_6)DMSO with an increasing amount of H_2O. As shown in *Fig. 3*, the signal of amide NH_a moved downfield from 7.24 to 7.42 ppm as the H_2O content increased up to 30%, and then shifted upfield from 7.42 to 7.34 ppm as the water content increased further to 40%. A similar phenomenon was observed for NH_b, the signal of which moved downfield from 8.00 to 8.26 ppm as the H_2O content increased up to 20%, and then shifted upfield from 8.26 to 7.95 ppm as the H_2O content increased to 40%. The changes in the chemical shifts of the amide H-atoms to lower fields for up to a 30% H_2O content and then upfield over 30% reveal that the H-bonding with (D_6)DMSO ($S{=}O\cdots H{-}N$) replaces that with H_2O ($H_2O\cdots H{-}N$), and then with intermolecular H-bonding between the amide groups. On the other hand, the chemical shift of the pyridinium H_c H-atoms shifted upfield (from 8.30 to 8.04 ppm) at 0 to 30% H_2O content, and then to lower field (from 8.04 to 8.14 ppm) at 40% H_2O. It indicated that the hydration of the charged pyridinium residues leads to the upfield shift when the H_2O content is below 30% and the dehydration of the charged pyridinium leads to the downfield shift if the H_2O content is higher than 30% [11]. Consequently, the

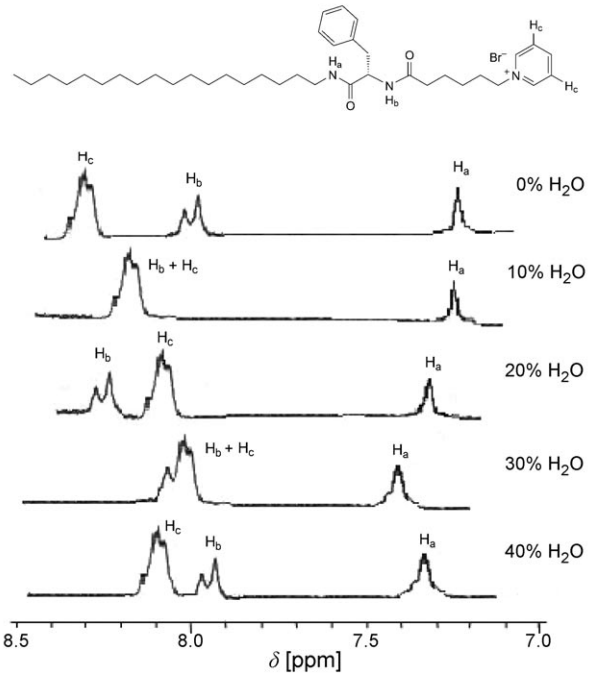

Fig. 3. *^{1}H-NMR Spectra of* **NP18PB** *in (D_6)DMSO with increasing H_2O content*

intermolecular H-bonding interaction is one of the main driving forces for the self-assembly of **NP18PB** molecules.

5. *Fluorescence Study.* To further characterize the hydrophobic interaction, the luminescence spectra were studied with 8-anilino-1-naphthalenesulfonic acid (ANS) as a probe. *Fig. 4,a* shows the typical luminescence spectra of ANS in aqueous solutions containing various concentrations of **NP18PB**, and *Fig. 4,b*, shows the dependence of the luminescence maxima (λ_{max}) and the relative luminescence intensities (I/I_0, where I_0 and I represent the luminescence intensities of ANS at λ_{max} in the absence and in the presence of **NP18PB**, resp.) on the concentration of **NP18PB**. At concentrations of

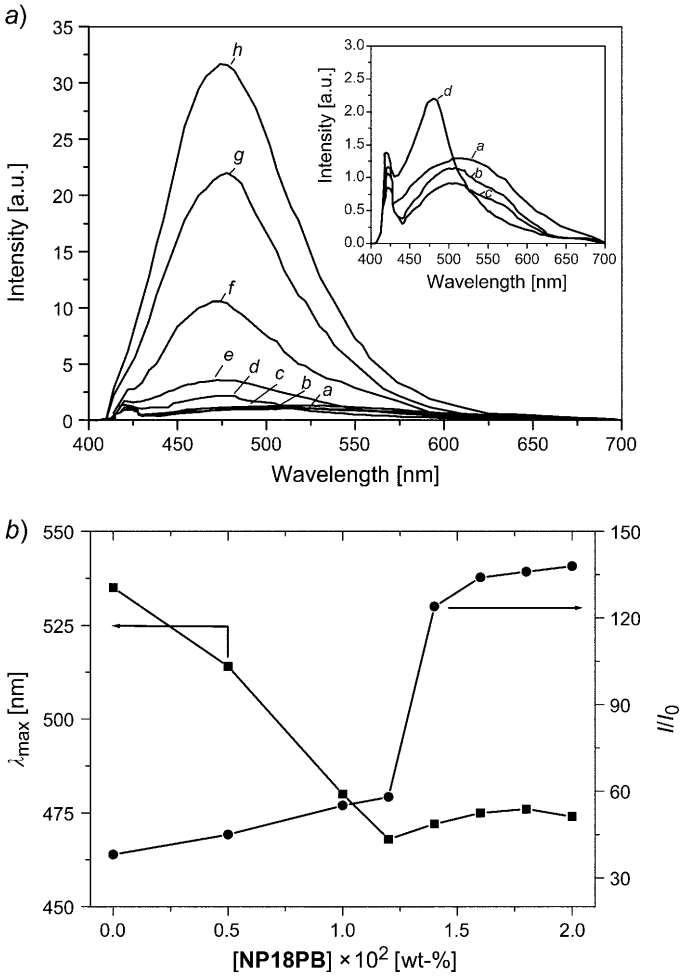

Fig. 4. *a*) *Luminescence spectra of ANS* (1.0×10^{-5} M) *in aqueous solutions containing various concentrations of* **NP18PB** *at room temperature.* Inset: enlargement of the low concentration range. *b*) *Dependence of the luminescence maxima* (λ_{max}; ■) *and relative luminescence intensities* (I/I_0; ●) *on the concentration of* **NP18PB**. [**NP18PB**] (× 100 wt-%): *a:* 0; *b:* 0.5; *c:* 1.0; *d:* 1.2; *e:* 1.4; *f:* 1.6; *g:* 1.8; *h:* 2.0.

NP18PB lower than 1.2 wt-%, **NP18PB** is dispersed in the solution. The exciplex through the interaction between **NP18PB** molecules is hardly formed resulting in a lower fluorescence intensity (*Fig. 4,a*). At a concentration of **NP18PB** at 1.2 wt-% or higher, the λ_{max} is blue-shifted from 535 nm to 468 nm with increasing **NP18PB** concentration. Further addition increases the relative luminescence intensity (*Fig. 4,b*), but produces only a slight change in the λ_{max} value (*Fig. 4,b*). Such luminescence behavior is frequently observed when the ANS molecules are incorporated into a hydrophobic environment; namely, the interior of the strands of self-assembled nanofibers is hydrophobic [12]. Therefore, this result indicated that one of the driving forces for the self-assembly of **NP18PB** into nanofibers is a hydrophobic interaction, which is in agreement with a previous report for amino acid based hydrogelators [13].

6. *Circular Dichroism* (CD). Circular dichroism (CD) spectra of **NP18PB** are shown in *Fig. 5*. A negative *Cotton* effect was observed in the amide absorption region, *i.e.*, at 220–225 nm, that could be attributed to the $\pi \rightarrow \pi$ transition of the amide bond along with a shoulder at longer wavelength from the $n \rightarrow \pi$ transition of the same bond [14]. These transitions are extremely sensitive to coupling with neighboring amides. The observed supramolecular chirality that emerged through noncovalent organized packing of molecular components was supported by a variable temperature CD study of **NP18PB** at 1.2 wt-%. The intensity of the CD peak at 220–225 nm gradually decreased with an increase in temperature from 25° to 80° as a result of the gel-to-solution state transition, leading to the destruction of the three-dimensional aggregate structure (*Fig. 2,a*). The results indicated that the chirality of the gelator is responsible for the formation of the self-assembled aggregates and supramolecular hydrogel.

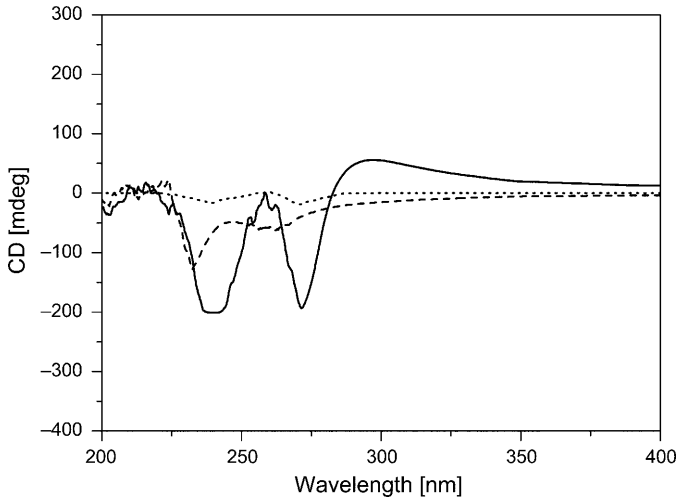

Fig. 5. *CD Spectra of* **NP18PB** *at 1.2 wt-% in plain H_2O with varying temperature from 20° to 80°, hydrogels* (solid line) *at 25°; loose hydrogels* (dashed line) *at 60°; homogeneous solution* (dotted line) *at 80°.*

7. *X-Ray Diffraction* (XRD) *Measurements.* The xerogel of **NP18PB** obtained from H_2O by a freezing method resulted in spongelike aggregates, instead of a typical crystalline solid. The X-ray diffraction patterns of the xerogel of **NP18PB** prepared from H_2O show periodical reflection peaks (*Fig. 6*), an indication that **NP18PB** indeed assembles into a lamellar organization. The obtained long spacings of the xerogel of **NP18PB** are 2.90 nm, 1.46 nm and 0.97 nm, corresponding to the ratio of 1 : 1/2 : 1/3 : 1. The 2.90 nm length is smaller than twice that of the extended molecular length of 1 (2.45 nm, by CPK molecular modeling), but larger than the length of one molecule. Thus, the aqueous gel of **NP18PB** should maintain an interdigitated bilayer structure with a thickness of 2.90 nm (*Fig. 6*). Long spacing of 2.90 nm was also observed for the aqueous gel state of **NP18PB** at high concentration. In addition, the wide-angle region of the X-ray diagram for the aqueous gel of **NP18PB** revealed a series of sharp reflection peaks, supporting the view that presumably long alkyl chain groups form highly ordered layer packing through the interdigitated hydrophobic interaction [9]. Thus, a rational model of the energy-minimized structure of **NP18PB** self-assembled in water is shown in *Fig. 7.*

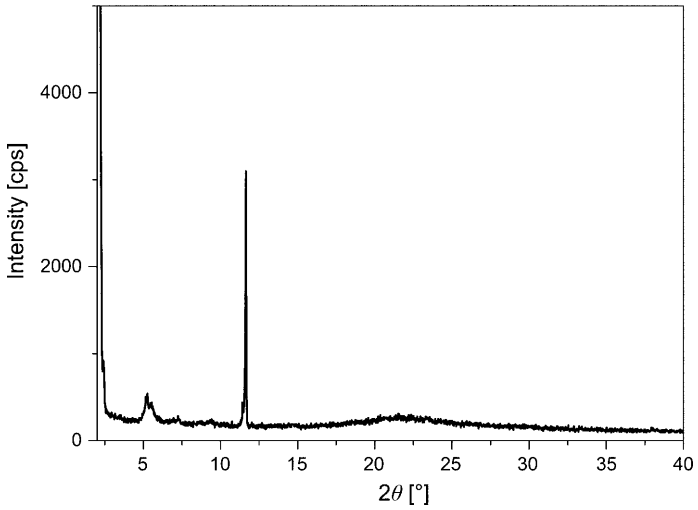

Fig. 6. *XRD Spectra of the gelator xerogel from hydrogel* (6.0 wt-%)

Conclusions. – We have synthesized a hydrogelator based on L-phenylalanine with a long hydrophobic chain and a positive charged terminus, *i.e.*, a pyridinium group. After dissolution of the hydrogelator in H_2O, it can gelate H_2O, and form a transparent hydrogel. ^{1}H-NMR, POM, FE-SEM, CD, XRD, and fluorescence studies demonstrated that the formation of the hydrogels by this hydrogelator involves two self-assembling processes, *i.e.*, the formation of some aggregates and their growth into nanofibers. Moreover, the driving forces for the self-assemblies are the hydrophobic interactions between the alkyl groups and H-bonding between the amide groups.

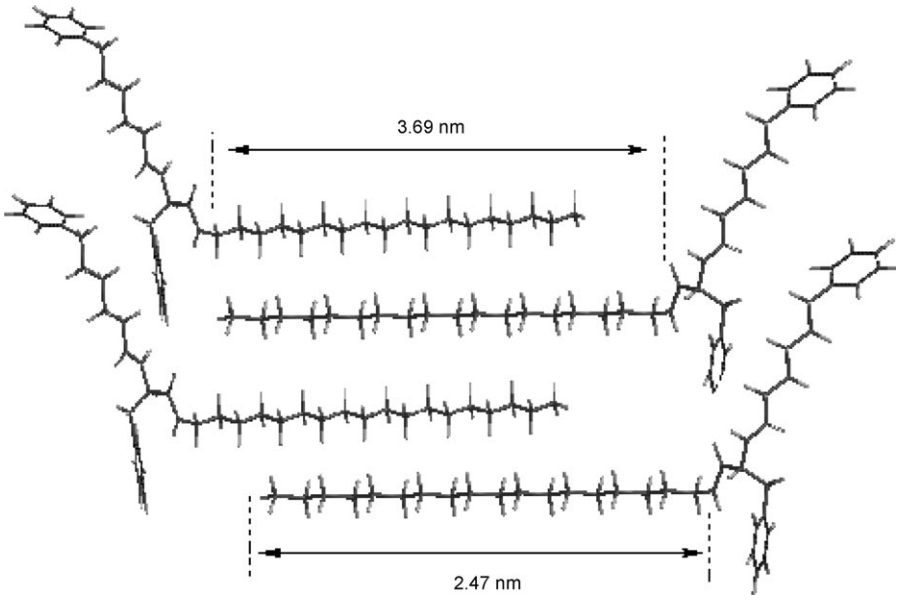

Fig. 7. *Model of the energy-minimized structure of hydrogelator self-assembled in water*

Experimental Part

General. L-Phenylalanine, bis(trichloromethy1) carbonate (BTC), *N*-octadecylamine, 6-bromohexanoyl chloride, and 8-anilinonaphthalene-1-sulfonic acid (ANS) were purchased from *Aldrich* and used as received. THF was dried over Na and distilled before use. Pyridine was distilled over NaOH, and CH_2Cl_2 was distilled over P_4O_{10}. Other solvents were distilled before use.

Synthesis of the Hydrogelator **NP18PB** (*Scheme*). *(4S)-4-Benzyl-1,3-oxazolidine-2,5-dione* (**L-Phe-NCA**). The starting material (4*S*)-4-benzyl-1,3-oxazolidine-2,5-dione (**L-Phe-NCA**) was synthesized according to a reported procedure [9]. M.p. 95–96° (dec.). FT-IR (KBr): 3285 (N–H, amide A), 1853, 1760 (C=O, ester), 1634 (C=O, amide I), 1554 (N–H, amide II). ^{1}H-NMR (400 MHz, $CDCl_3$): 7.46–7.21 (*m*, 5 arom. H); 6.42 (*s*, 1 NH); 4.55–4.32 (*m*, 1 H–C); 3.36–2.88 (*m*, CH_2–Ar). Anal. calc. for $C_{10}H_9NO_3$ (191.19): C 62.83, H 4.75, N 7.32; found: C 62.73, H 4.73, N 7.34.

N-*Octadecyl*-L-*phenylalaninamide* (**C_{18}Phe**). Octadecylamine (3.57 g, 13.3 mmol) and **L-Phe-NCA** (2.54 g, 13.3 mmol) were dissolved in 50 ml of CH_2Cl_2 and cooled in an ice bath. The mixture was stirred for 1 h and then at 40° for 72 h. The product *N*-octadecyl-L-phenylalaninamide (**C_{18}Phe**) was precipitated from Et_2O. FT-IR (KBr): 3284 (N–H, amide A), 1634 (C=O, amide I), 1554 (N–H, amide II). ^{1}H-NMR (400 MHz, $CDCl_3$): 8.24 (*s*, NH_2); 8.20 (*d*, *J* = 7.6, NH_2 or NH); 7.33–7.19 (*m*, 5 arom. H (Ph)); 3.88–3.69 (*m*, PhCH_2C*H*); 3.29–3.16 (*m*, CH_2CH_2NH); 3.13–2.90 (*m*, PhCH_2); 2.20–2.13 (*m*, CH_2Me); 1.31–1.16 (*m*, 30 H, CH_2(CH_2)$_{15}$CH_2Me); 0.84 (*t*, *J* = 6.8, CH_2CH_2*Me*). Anal. calc. for $C_{27}H_{48}N_2O$ (416.69): C 77.83, H 11.61, N 6.72; found: C 77.74, H 11.64, N 6.76.

N$^{\alpha}$-*(6-Bromohexanoyl)*-N-*octadecyl*-L-*phenylalaninamide* (**NP18**). After drying in vacuum, **C_{18}Phe** (4.87 g, 11.3 mmol) and 4.68 ml of Et_3N were added to 300 ml of anh. THF. 6-Bromohexanoyl chloride (2.66 g, 12.5 mmol) was added dropwise to the mixture at 0°. The reaction was carried out at 0° for 1 h and then at r.t. for 4 h. After evaporating THF, *N*$^{\alpha}$-(6-bromohexanoyl)-*N*-octadecyl-L-phenylalaninamide (**NP18**) was obtained and recrystallized from EtOH, and dried in vacuum. FT-IR (KBr): 3284 (N–H, amide A), 1634 (C=O, amide I), 1554 (N–H, amide II). ^{1}H-NMR (400 MHz, $CDCl_3$, TMS): 7.48 (*d*, *J* = 7.8, NH); 7.35–7.17 (*m*, 5 arom. H (Ph)); 6.60 (*t*, *J* = 5.6, NH); 3.4 (*t*, *J* = 4.4, CH_2Br); 3.28–3.15 (*m*, CH_2CH_2NH); 3.14–3.06 (*m*, PhCH_2C*H*); 3.03–2.88 (*m*, PhCH_2); 2.57–2.48 (*m*, NHCOCH_2);

2.20–2.13 (*m*, CH_2CH_2Me); 1.30–1.25 (*m*, $CH_2(CH_2)_{15}CH_2Me$, $CH_2(CH_2)_3CH_2Br$); 0.88 (*t*, *J* = 6.8, *Me*). Anal. calc. for $C_{33}H_{57}BrN_2O_2$ (593.73): C 66.76, H 9.68, Br 13.46, N 4.72; found: C 66.87, H 9.65, Br 13.41, N 4.70.

N-*Octadecyl*-N$^{\alpha}$-*[6-(pyridinium-1-yl)hexanoyl]*-L-*phenylalaninamide Bromide* (**NP18PB**). **NP18** (3.5 g, 5.5 mmol) was refluxed in 50 ml of pyridine under N_2 atmosphere overnight. The mixture was evaporated and recrystallized from a mixture of EtOH and acetone. The final product *N*-octadecyl-*N*$^{\alpha}$-[6-(pyridinium-1-yl)hexanoyl]-L-phenylalaninamide bromide (**NP18PB**) was obtained. FT-IR: 3284 (N–H, amide A), 1634 (C=O, amide I), 1546 (N–H, amide II). ^{1}H-NMR (400 MHz, $CDCl_3$): 9.54 (*d*, *J* = 5.6, 2 H–C(2_{Py})); 8.52 (*t*, *J* = 7.8, H–C(4_{Py})); 8.31 (*t*, *J* = 7.4, 2 H–C(3_{Py})); 7.73 (*d*, *J* = 7.4, NH); 7.35–7.17 (*m*, 5 arom. H (Ph)); 6.76 (*t*, *J* = 5.5, NH); 3.27–3.13 (*m*, $PhCH_2$); 3.18–3.16 (*m*, CH_2CH_2NH); 3.03–2.88 (*m*, $PhCH_2CH$); 2.23–2.03 (*m*, $CH_2CH_2N^+Br^-$); 2.2–2.13 (*m*, CH_2Me); 1.31–1.25 (*m*, $CH_2(CH_2)_{15}CH_2Me$, $CH_2(CH_2)_3CH_2N^+$); 0.88 (*t*, *J* = 6.8, CH_2Me). Anal. calc. for $C_{38}H_{62}BrN_3O_2$ (672.83): C 67.84, H 9.29, Br 11.87, N 6.25; found: C 67.96, H 9.23, Br 11.84, N 6.23.

FT-IR Spectra: *Fourier* transform infrared (FT-IR) spectra were recorded on *EQUINOX55* spectrophotometer (KBr pellets). ^{1}H-NMR Spectra: solns. of **NP18PB** (1.5 wt-%) were prepared in (D_6)DMSO containing various ratios of H_2O, namely, 0, 10, 20, 30, and 40%.

Polarized Optical Microscope. The optical analysis of the hydrogels was performed by using a polarized optical microscope (POM, *BH-2*). The soln. containing 2 wt-% of **NP18PB** was dropped on a pre-warmed glass plate and allowed to cool to r.t. The hydrogel samples were kept at r.t. for 4–6 h before testing.

Field Emission Scanning Electron Microscopy (FE-SEM, *Sirion 200*, FEI). The gel samples were frozen by liquid N_2 and then freeze-dried. The fractured specimens were coated with Au. The electric current was 15 mA, and the accelerating voltage was 5 kV.

Fluorescence Spectroscopy. The steady-state fluorescence spectra were recorded with an *FP-6500* spectrofluorometer. Fluorescence spectra were measured at [ANS] = 1.0×10^{-5} M and [gelator] = 0–2.0 wt-% in a fluorescence spectroscopic cell (1 cm × 1 cm). The excitation wavelength was 360 nm, corresponding to the absorption maximum.

Circular Dichroism (CD). The CD spectra of an aq. soln. of **NP18PB** at 1.2 wt-% with varying temp. from 20° to 80° were recorded by using a quartz cuvette of 1 mm path length with a *Jasco* spectropolarimeter.

X-Ray Diffraction (XRD). XRD measurements were taken with an *X'Pert PRO* diffractometer, and the source was CuK_{α} radiation (α = 0.15406 nm) with a voltage and current of 40 kV and 30 mA, resp. Hydrogels of **NP18PB** were mounted on the aluminum holder and scanned from 2 to 40°.

Gelation and Minimum Gelator Concentrations (MGC). The weighed hydrogelator **NP18PB** was mixed with 3 ml of H_2O in a test tube, and the mixture was heated until the solid was completely dissolved. The soln. was allowed to cool to r.t. for 12 h and exhibited no gravitational flow upon inversion of the test tube. A required minimum amount of **NP18PB** gelation is defined as minimum gelation concentration (MGC) [10].

The Phase Dissociation Temp. (T_{GS}). A small steel ball (250 mg, ∅ 4 mm) was placed on top of the supramolecular hydrogel in a test tube (∅ 10 mm). Then the sample was slowly heated (2°/min) in a thermostatted water bath. When the ball fell to the bottom of the test tube, the temp. was defined as the phase dissociation temp. (T_{GS}) of the supramolecular hydrogels [15].

The work was financially supported by the *National Natural Science Foundation of China* (No. 20474022) and *Scientific Research Program* of the Education Department of Henan Province, China (No. 2008B430014).

REFERENCES

[1] P. Terech, R. G. Weiss, *Chem. Rev.* **1997**, *97*, 3133; D. J. Abdallah, R. G. Weiss, *Adv. Mater.* **2000**, *12*, 1237.

[2] D. Das, A. Dasgupta, S. Roy, R. N. Mitra, S. Debnath, P. K. Das, *Chem.–Eur. J.* **2006**, *12*, 5068; M. Suzuki, M. Yumoto, H. Shirai, K. Hanabusa, *Chem.–Eur. J.* **2008**, *14*, 2133.

[3] K. Köhler, G. Förster, A. Hauser, B. Dobner, U. F. Heiser, F. Ziethe, W. Richter, F. Steiniger, M. Drechsler, H. Stettin, A. Blume, *Angew. Chem., Int. Ed*. **2004**, *43*, 245; K. Köhler, G. Förster, A. Hauser, B. Dobner, U. F. Heiser, F. Ziethe, W. Richter, F. Steiniger, M. Drechsler, H. Stettin, A. Blume, *J. Am. Chem. Soc*. **2004**, *126*, 16804.
[4] F. M. Menger, K. L. Caran, *J. Am. Chem. Soc*. **2000**, *122*, 11679; S. Mukhopadhyay, U. Maitra, Ira, G. Krishnamoorthy, J. Schmidt, Y. Talmon, *J. Am. Chem. Soc*. **2004**, *126*, 15905.
[5] a) M. Suzuki, M. Yumoto, M. Kimura, H. Shirai, K. Hanabusa, *Chem.–Eur. J.* **2003**, *9*, 348; b) L. A. Estroff, A. D. Hamilton, *Angew. Chem., Int. Ed.* **2000**, *39*, 3447.
[6] a) A. Motulsky, M. Lafleur, A.-C. Couffin-Hoarau, D. Hoarau, F. Boury, J.-P. Benoit, J.-C. Leroux, *Biomaterials* **2005**, *26*, 6242; b) M. Moniruzzaman, P. R. Sundararajan, *Langmuir* **2005**, *21*, 3802.
[7] M. Suzuki, T. Sato, A. Kurose, H. Shirai, K. Hanabusa, *Tetrahedron Lett.* **2005**, *46*, 2741; M. Suzuki, S. Owa, M. Kimura, A. Kurose, H. Shirai, K. Hanabusa, *Tetrahedron. Lett*. **2005**, *46*, 303.
[8] X. Fu, N. Wang, S. Zhang, H. Wang, Y. Yang, *J. Colloid Interface Sci.* **2007**, *315*, 376.
[9] J. G. Nery, G. Bolbach, I. Weissbuch, M. Lahav, *Chem.–Eur. J.* **2005**, *11*, 3039.
[10] K. Hanabusa, K. Okui, K. Karaki, M. Kimura, H. Shirai, *J. Colloid Interface Sci.* **1997**, *195*, 86.
[11] S. Masahiro, Y. Mariko, K. Mutsumi, S. Hirofusa, K. Hanabusa, *Angew. Chem., Int. Ed.* **2003**, *19*, 348.
[12] L. E. Bromberg, D. P. Barr, *Macromolecules* **1999**, *32*, 3649.
[13] Z. Yang, B. Xu, *Chem. Commun.* **2004**, 2424.
[14] M. George, G. Tan, V. T. John, R. G. Weiss, *Chem.–Eur. J.* **2005**, *11*, 3243.
[15] A. Carré, P. Le Grel, M. Baudy-Floch, *Tetrahedron Lett.* **2001**, *42*, 1887.

Received April 22, 2009